Int J Clin Exp Pathol 2016;9(2):639-650
www.ijcep.com /ISSN:1936-2625/IJCEP0019988

Original Article

Knockdown of ATPase family AAA domain-containing protein 2 inhibits the proliferation of colorectal cancer cells *in vitro* and *in vivo*

Sen Hong[1,2*], Miaomiao Bi[3*], Si Chen[2], Di Sun[2], Limian Ling[2], Chunyan Zhao[1], Lei Wang[2]

[1]Department of Physiology, College of Basic Medical Sciences, Jilin University, Changchun, Jilin, China; [2]Department of Colorectal and Anal Surgery, The First Hospital of Jilin University, Changchun, Jilin, China; [3]Department of Ophthalmology, China-Japan Union Hospital of Jilin University, Changchun, Jilin, China. [*]Equal contributors.

Received November 18, 2015; Accepted January 24, 2016; Epub February 1, 2016; Published February 15, 2016

Abstract: ATPase family AAA domain-containing protein 2 (ATAD2) has been reported to be associated with the development of many malignant cancers. Our study firstly investigated the functional roles of ATAD2 gene in colorectal cancer (CRC) *in vitro* and *in vivo*. Here, Caco-2 and SW480 cell lines were transfected with ATAD2 short hairpin RNA (shRNA) plasmid to silence ATAD2 expression, as measured by real-time PCR and western blot. Cell proliferation and cell cycle distribution *in vitro* were determined by CCK-8, colony formation assay and flow cytometry. The effect of ATAD2 knockdown on tumor growth and tumor weight was evaluated in BALB/c-nude mice *in vivo*. Meanwhile, proliferation-related and cell cycle-related proteins were examined by real-time PCR, western blot and immunohistochemistry (IHC). Our results demonstrated that ATAD2 knockdown significantly inhibited cell proliferation and arrested cell cycle at the G1 phase. Decreased levels of c-myc, proliferating cell nuclear antigen (PCNA), Ki67, phosphorylated (p)-Akt, Akt, cyclin D1, cyclin E1 and cyclin-dependent kinase 2 (CDK2) were detected after ATAD silencing, whereas p21 expression was increased. Moreover, administration of shATAD2 plasmid significantly suppressed tumor growth and reduced tumor weight in nude mice, with the decreased levels of ATAD2, PCNA, c-myc and Ki67 in tumor tissues. The results suggest that ATAD2 may play crucial roles in CRC development. Targeting ATAD2 may be an efficient therapeutic approach in CRC treatment.

Keywords: ATAD2, colorectal cancer, short hairpin RNA, cell cycle arrest, tumor growth

Introduction

Colorectal cancer (CRC) is one of the most common malignant cancers worldwide ranking the second in females and the third in males [1, 2]. It causes nearly 600,000 people die of CRC annually [3]. When the people were diagnosed with CRC, tumors from approximately 60% of the patients were resectable [4]. Currently, surgical resection combined with chemotherapy is considered as the optimal strategy for the treatment of CRC [4, 5]. Despite the improvement in the diagnosis and treatment of CRC, the overall survival rate remains stubbornly low [6]. Tumor metastasis and recurrence after surgical resection are still the leading causes of its high mortality [7]. Therefore, there is an urgent need for studying the mechanism of CRC occurrence and development and seeking an effective therapeutic strategy for the treatment of CRC.

ATPase family AAA domain-containing protein 2 (ATAD2) is a protein containing ATPase domain and a bromodomain [8]. ATAD2 is an important co-activator for numerous transcription factors (MYC and E2F family members) and regulates the expression of proliferation-related genes [9]. Several previous findings have found that ATAD2 is highly expressed in lung cancer, breast cancer and hepatocellular carcinoma [10]. Elevated expression level of ATAD2 leading to poor outcomes in multiple cancers [11-13]. RNA interference (RNAi) is a gene-silencing system that inactivates homology-dependent genes in eukaryotic organisms [14]. Downregulation of ATAD2 expression using RNAi technology suppresses the proliferation and invasion of cancer

cells and promotes cell apoptosis [9, 10, 15, 16].

In order to investigate the roles of ATAD2 in the biological behavior of CRC, we constructed ATAD2 short hairpin RNA (shRNA) recombinant plasmid and then they were transfected into Caco-2 and SW480 to inhibit the endogenous gene expression of ATAD2. Next, the transfection efficiency was examined. The impact of ATAD2 knockdown on proliferation, colony formation and cell cycle of CRC cell lines *in vitro* and tumor growth *in vivo* were investigated.

Materials and methods

Cell lines

Colorectal cancer (CRC) cell lines Caco-2 and SW480 were obtained from cell bank at Chinese Academy of Sciences (Shanghai, China). The cells were cultured in DMEM (Dulbecco's Modified Eagle Medium) (Gibco, Grand Island, NY, USA) supplemented with 10% FBS (fetal bovine serum) (Hyclone, Logan, UT, USA) at 37°C in a 5% CO_2 atmosphere.

Construction of eukaryotic expression plasmid and transfection

Specific short hairpin RNA (shRNA) sequences against ATAD2 and non-silencing sequence that served as a negative control were purchased from Wanleibio (Shenyang, China) and subcloned into the restriction sites of eukaryotic expression vector pRNA-H1.1 (GenScript, Nanjing, China) via *Bam*H I and *Hin*d III. The shRNA sequences were: shATAD2 5'-GATCCCCGGCGATGGGTCATCAGTTATTCAAGAGATAACTGATGACCCATCGCCTTTTT-3' and 5'-AGCTAAAAAGGCGATGGGTCATCAGTTATCTCTTGAATAACTGATGACCCATCGCCGGG-3'; shCtr 5'-GATCCCCTTCTCCGAACGTGTCACGTTTCAAGAGAACGTGACACGTTCGGAGAATTTTT-3' and 5'-AGCTAAAAATTCTCCGAACGTGTCACGTTCTCTTGAAACGTGACACGTTCGGAGAAGGG-3'. Caco-2 and SW480 cells were seeded in 6-well plates (at a density of 3×10^5 cells/well). After 24 h of cell culture, the cells were transfected with shRNA plasmids or negative control using Lipofectamine 2000 (Invitrogen, Grand Island, NY, USA). At 24 h post-transfection, stable single clones were selected using G418 solution (Invitrogen). The expression levels of ATAD2 were measured by real-time PCR and western blot.

Real-time PCR analysis

Total RNAs were isolated from the cells and tumor tissues using total RNA kit (BioTeke, Beijing, China) according to the instructions of the manufacturer and the concentration was determined using a spectrophotometer (Model NanoDrop 2000, Thermo Scientific, Grand Island, NY, USA). Subsequently, cDNAs were synthesized from the isolated RNAs (1 μg) using M-MLV Reverse Transcriptase (BioTeke). The primers used in the present study were: ATAD2-Forward 5'-TGGGAAATAGTTGGACCGACAC-3' and Reverse 5'-TTCTGGCAAAGCGGAATGG-3'; PCNA-Forward 5'-CCTGTAGCGGCGTTGTTGC-3' and Reverse 5'-GTCGCAGCGGTAGGTGTCG-3'; Ki67-Forward 5'-ATCGAACACCAGCTAAAGT-3' and Reverse 5'-CAGGTAACCCAGAGCACAT-3'; CDK2-Forward 5'-AGAAACAAGTTGACGGGAGA-3' and Reverse 5'-GGAAGAGGAATGCCAGTGAG-3'; Akt-Forward 5'-GAAGAAGCTCAGCCCACCCTT-3' and Reverse 5'-AAGCTATCGTCCAGCGCAGTC-3'; c-myc-Forward 5'-GGAGGCTATTCTGCCCATTT-3' and Reverse 5'-AGGTCATAGTTCCTGTTGGTG-3'; cyclin D1-Forward 5'-CCCGCACGATTTCATTGAAC-3' and Reverse 5'-AGGGCGGATTGGAAATGAAC-3'; cyclin E1-Forward 5'-GCCTTGTATCATTTCTCGTCA-3' and Reverse 5'-TGGGTCTGTATGTTGTGTGC-3'; p21-Forward 5'-CTGTCACTGTCTTGTACCCTTGT-3' and Reverse 5'-CTTCCTGTGGGCGGATTAG-3'; β-actin-Forward 5'-CTTAGTTGCGTTACACCCTTTCTTG-3' and Reverse 5'-CTGTCACCTTCACCGTTCCAGTTT-3'. Real-time PCR was performed using SYBR Green dye (Solarbio, Beijing, China) on a Real-time Quantitative Thermal Block (Bioneer, Daejeon, Korea): 95°C for 10 min; 95°C for 10 s, 60°C for 20 s, 72°C for 30 s, a total of 40 cycles; 4°C for 5 min. The relative gene expression was determined using the $2^{-\Delta\Delta Ct}$ [17].

Western blot analysis

Tumor tissues and the cells were homogenized in ice-cold Radio Immunoprecipitation Assay (RIPA) lysis buffer (Beyotime, Haimen, China). RIPA buffer contained 1% protease inhibitor phenylmethanesulfonyl fluoride (PMSF) (Beyotime). After placed on ice for 5 min, they were centrifuged at 12000 rpm for 10 min. The supernatant was the total protein extraction. The extracted proteins were then subjected to SDS-PAGE (sodium dodecyl sulfate polyacrylamide gel electrophoresis) and transferred to Millipore PVDF (polyvinylidene fluoride) mem-

branes (Millipore, Billerica, MA, USA). The membranes were incubated with antibodies against ATAD2 (#ab176319, 1:1000, Abcam, Cambridge, MA, USA), c-myc (#sc-40, 1:200, Santa Cruz, Dallas, Texas, China), PCNA (#sc-25280, 1:200, Santa Cruz), Ki67 (#sc-15402, 1:200, Santa Cruz), Akt (#sc-8312, 1:200, Santa Cruz), p-Akt (#sc-135651, 1:200, Santa Cruz), cyclin D1 (#BM0771, 1:400, Boster, Wuhan, China), cyclin E1 (#BA0774, 1:400, Boster), CDK2 (#BA0463, 1:400, Boster) and p21 (#BA0272, 1:400, Boster) overnight at 4°C and then with horseradish peroxidase (HRP)-conjugated goat anti-rabbit/mouse IgG (#A0208, #A0216, 1:5000, Beyotime) at 37°C for 45 min. The relative densities of protein bands were analyzed using enhanced chemiluminescence (ECL) reagent (Wanleibio).

Cell proliferation assay

The cells in each group were counted, plated in 96-well plates (3×10^3 cells/well) at cultured at 37°C. After 0, 24, 48, 72 and 96 h, CCK-8 solution (7Sea, Shanghai, China) was added to incubate with the cells for 1 h. The absorbance at OD_{450} was measured using a model ELX-800 microplate reader (Bio-Tek, Winooski, VT, USA).

Colony formation assay

The cells were seeded on 35 mm culture dishes. Each culture dish contained 200 cells. After cultured at 37°C for 1 week, the cells were fixed with paraformaldehyde (Sinopharm, Shenyang, China) at room temperature for 20 min. After washed with PBS, the cells were stained with Wright-Giemsa Stain (Jiancheng, Nanjing, China) for 5-8 min and counted under a microscope (AE31, Motic, Xiamen, China). A colony that contained more than 50 cells was counted as a colony. The colony formation rate was calculated using the formula: Colony formation rate = (colony numbers/the number of seeded cells) × 100%.

Cell cycle analysis

Cell cycle distribution was analyzed by flow cytometry (BD, Franklin Lakes, NJ, USA) using a cell cycle analysis kit (Beyotime) according to the manufacturer's instructions. Briefly, the cells were harvested by centrifugation (2000 rpm for 5 min) after shRNA transfection. The cells were washed with PBS and fixed with 70% ethanol for 2 h at 4°C. Subsequently, the cells were resuspended in staining buffer, incubated with propidium iodide (PI) (at 37°C for 30 min) and analyzed later.

Xenograft model

Female BALB/c-nude mice (4-6 weeks old) were purchased from Vital River (Beijing, China) and housed in a cage with a 12-h light/dark cycle. The mice were fed *ad libitum*. The mice were divided into two groups (8 mice/group): the shCtr group and the shATAD2 group. The mice in the shCtr group were subcutaneously injected with 1×10^7 SW480 cells that transfected with negative control shRNA plasmid. The mice in the shATAD2 group were injected with equal numbers of SW480 cells that transfected with ATAD2 shRNA plasmid. All animal experiments were performed according to guidelines approved by Institutional Animal Ethics Committee of Jilin University. Tumor length (L) and width (W) was measured using a caliper every 3 days. After 28 days, tumor tissues were excised and weighted. The tumor volume was calculated using the formula: Tumor volume = $1/2 \times L \times W^2$.

Immunohistochemistry (IHC)

Paraffin-embedded tumor tissues were cut into 5 μm sections (Model RM2235; Leica, Wetzlar, Germany). Then, the sections were deparaffinized in xylene and rehydrated. After antigen-retrieval, the slides were incubated with 3% hydrogen peroxide (H_2O_2) (Sinopharm) for 15 min at room temperature. Subsequently, the slides were blocked with goat serum and incubated with ATAD2 antibody (#ab154139, 1:200, Abcam) and Ki67 antibody at 4°C overnight (#sc-15402, 1:50, Santa Cruz) and then with biotin-conjugated goat anti-rabbit/mouse secondary antibody (#A0286, #A0277, 1:200, Beyotime). After washed with PBS, the slides were incubated with horseradish peroxidase (HRP)-conjugated avidin (#A0303, Beyotime) at 37°C for 30 min and reacted with 3,3'-diaminobenzidine (DAB). The sections were counterstained with hematoxylin (Solarbio) and photographed under a microscope (DP73; Olympus, Tokyo, Japan).

Statistical analysis

Data are expressed as the mean ± SD. The statistical analysis was determined by one-way

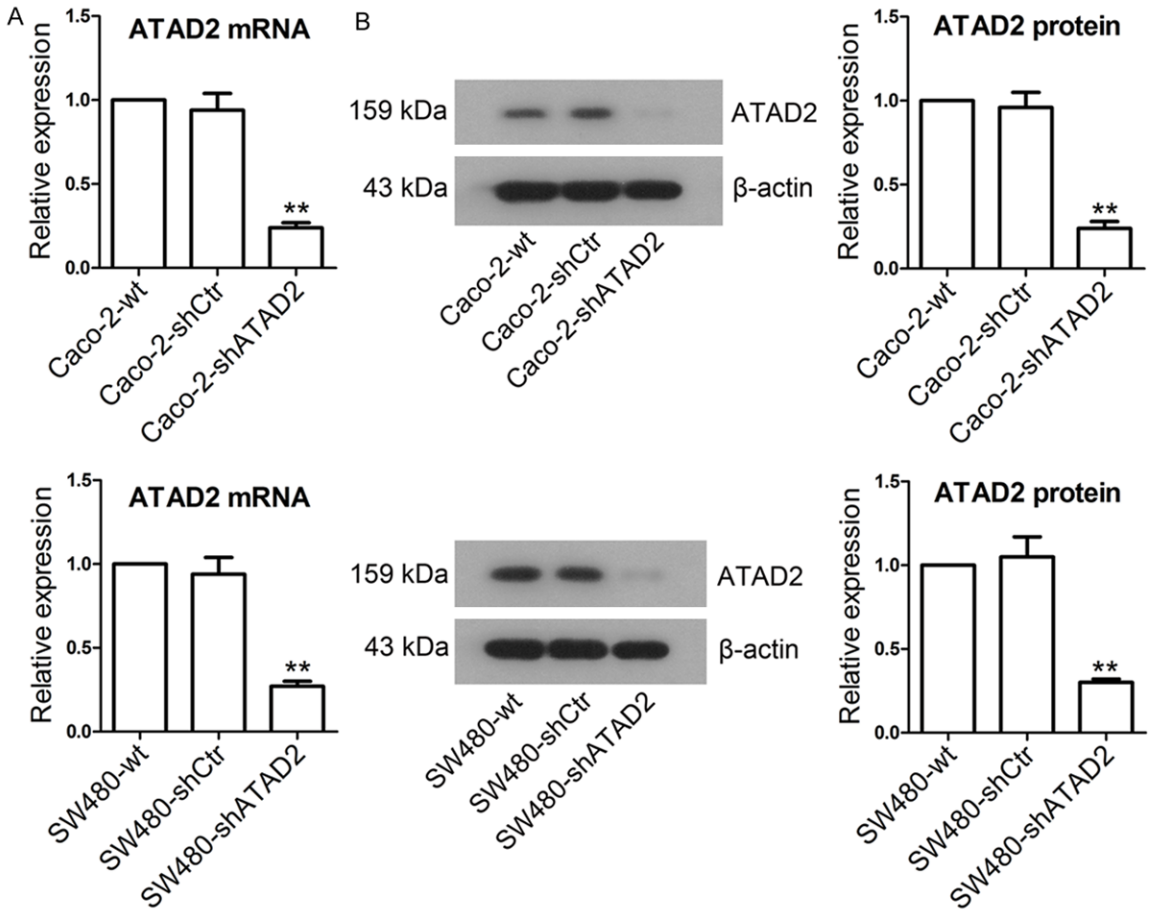

Figure 1. Knockdown of *ATAD2* gene expression in Caco-2 and SW480 cells. The cells were transfected with shATAD2 plasmid and shCtr plasmid, respectively. A. The levels of ATAD2 mRNA in both Caco-2 and SW480 cells were measured by real-time PCR. B. The levels of ATAD2 protein in both Caco-2 and SW480 cells were measured by western blot. β-actin was used as a loading control. Each value is the mean ± SD, n = 3. ***P*<0.01 *vs*. the shCtr group.

analysis of variance (ANOVA) and *Bonferroni post-hoc test* using GraphPad Prism software version 5.0 (GraphPad Software Inc., San Diego, CA, USA). *P*<0.05 was considered statistically significant.

Results

ATAD2 knockdown by ATAD2 shRNA

To evaluate the transfection efficiency of ATAD2 shRNA, real-time PCR and western blot was performed to measure the expression levels of ATAD2. As shown in **Figure 1A**, Caco-2-shATAD2 and SW480-shATAD2 groups showed a significant decrease in the levels of ATAD2 mRNA when compared with the shCtr group (*P*<0.01). As expected, ATAD2 knockdown greatly reduced the levels of ATAD2 protein in both Caco-2 and SW480 cell lines (**Figure 1B**, *P*<0.01).

ATAD2 knockdown inhibited cell proliferation and colony formation in vitro

The results showed that ATAD2 knockdown significantly lowered the proliferation capacity of Caco-2 and SW480 cells compared with the cells transfected with vector and untransfected cells (**Figure 2A**) (24, 48, 72 and 96 h, *P*<0.05). The results of colony formation assay showed that the colony-formation abilities of Caco-2-shATAD2 cells and SW480-shATAD2 cells were markedly lower than that of the shCtr group (**Figure 2B**, *P*<0.01). We then measured the changes of related genes. We found that ATAD2 knockdown significantly suppressed the expression of PCNA, c-myc, Ki67, Akt and p-Akt in both Caco-2 and SW480 cells, as demonstrated by real-time PCR (**Figure 3A**, *P*<0.01) and western blot (**Figure 3B**, *P*<0.01).

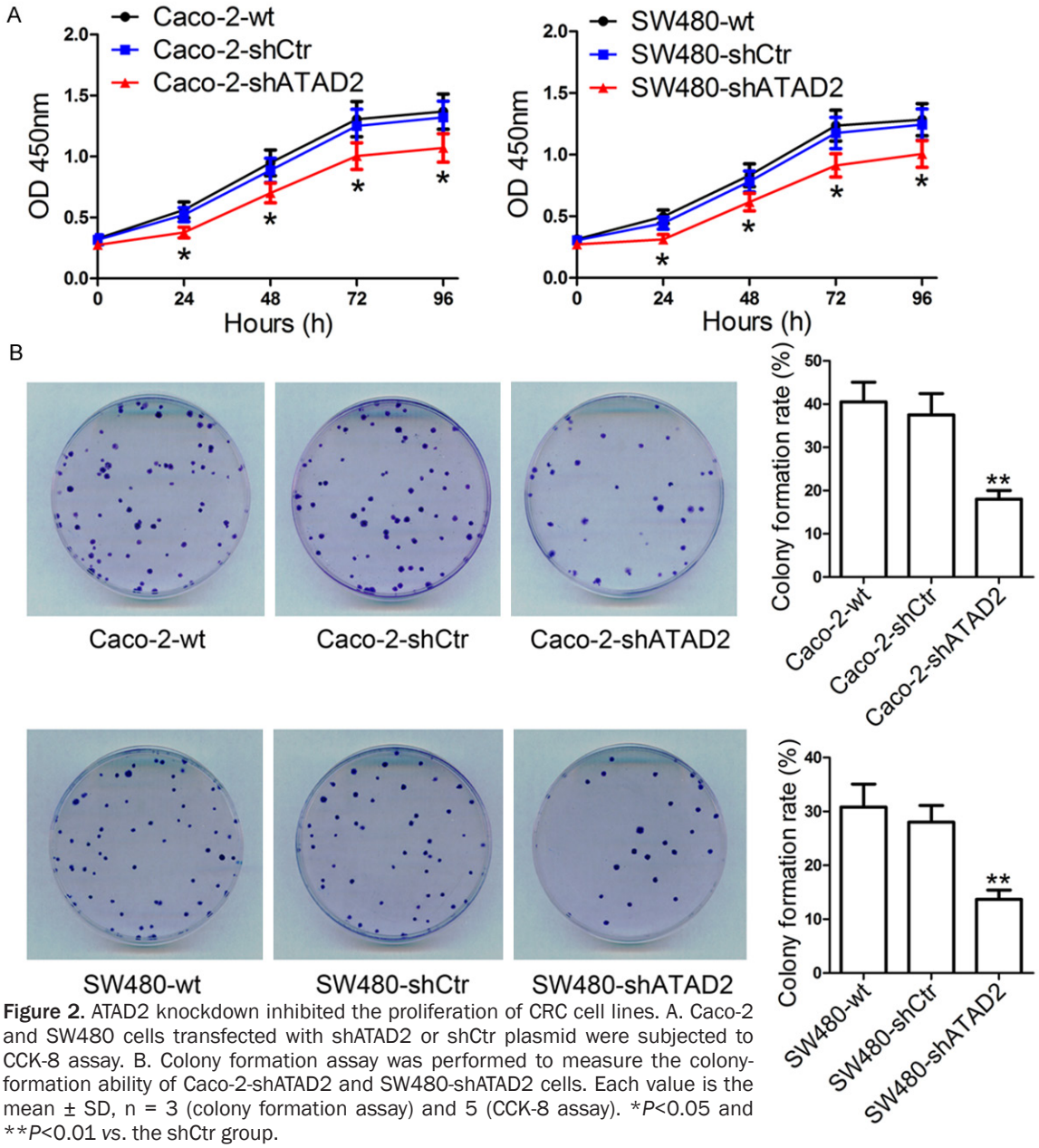

Figure 2. ATAD2 knockdown inhibited the proliferation of CRC cell lines. A. Caco-2 and SW480 cells transfected with shATAD2 or shCtr plasmid were subjected to CCK-8 assay. B. Colony formation assay was performed to measure the colony-formation ability of Caco-2-shATAD2 and SW480-shATAD2 cells. Each value is the mean ± SD, n = 3 (colony formation assay) and 5 (CCK-8 assay). **P*<0.05 and ***P*<0.01 *vs*. the shCtr group.

ATAD2 knockdown arrested cells in the G1 phase

Cell cycle arrest might cause the inhibition of cell proliferation. Therefore, cell cycle distribution was evaluated by flow cytometry in our study. As shown in **Figure 4**, the percentages of cells at the G1 phase in the Caco-2-shATAD2 group and SW480-shATAD2 group were significantly higher than that in the vector group (*P*<0.05). ATAD2 knockdown greatly decreased the proportions of G2 phase cells in the Caco-2-shATAD2 group (*P*<0.01) and S phase cells (*P*<0.05) in the SW480-shATAD2 group. Real-time PCR analysis demonstrated that cyclin D1, cyclin E1 and CDK2 mRNA levels were markedly reduced in both Caco-2 and SW480 cells after ATAD2 shRNA transfection (**Figure 5A**, *P*<0.01). We further measured the levels of CDK inhibitor p21. The results showed that p21 mRNA levels in the Caco-2 and SW480 cells were significantly elevated after knockdown of ATAD2 (*P*<0.01). Western blot further confirmed the changes of these proteins (**Figure 5B**, *P*<0.01).

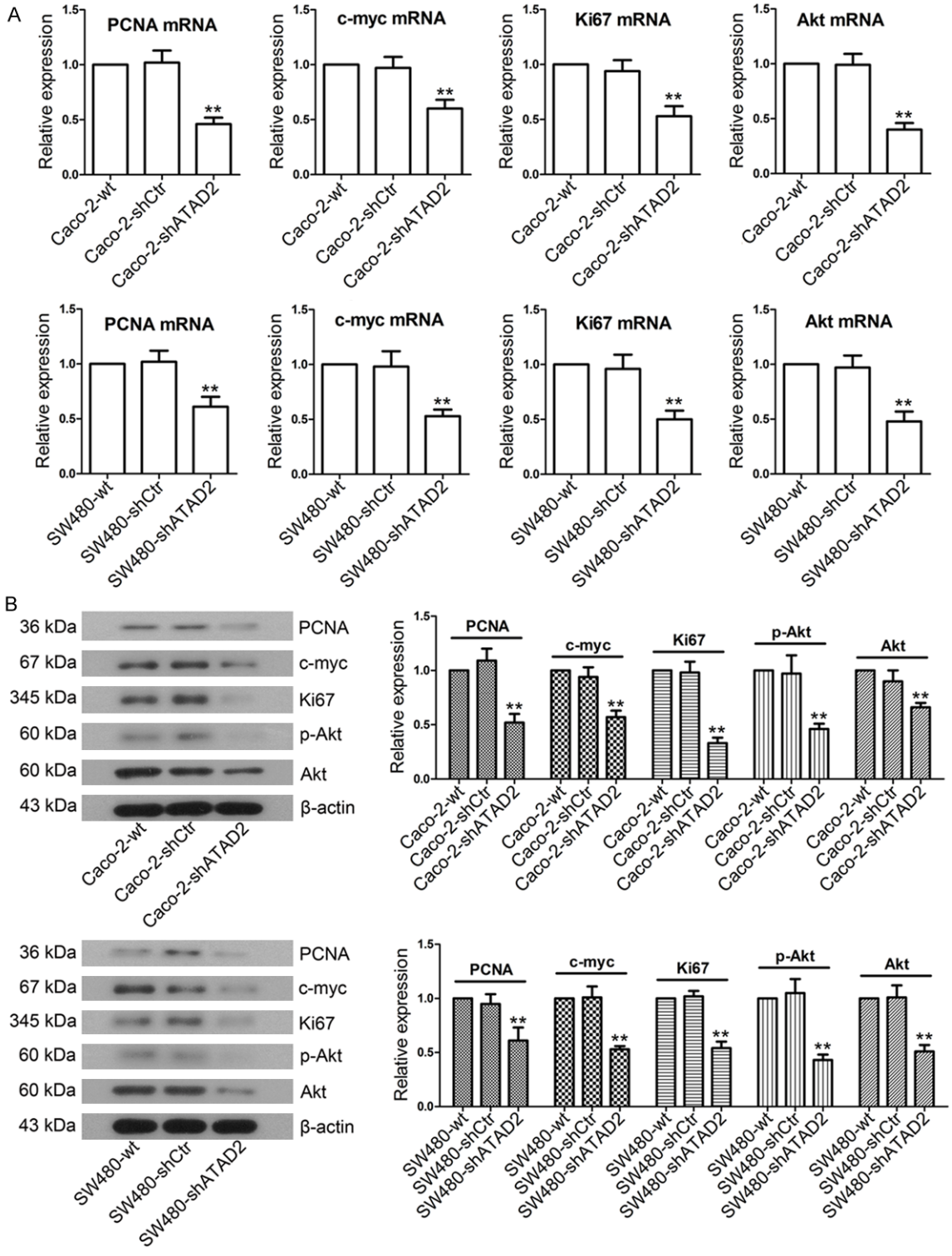

Figure 3. Effect of ATAD2 knockdown on the expression of proliferation-related genes. A. Total RNAs were extracted from the cells in each group. Subsequently, the mRNA levels of PCNA, c-myc, Ki67 and Akt were measured by real-time PCR. B. The protein levels of PCNA, c-myc, Ki67, p-Akt and Akt were analyzed by western blot. β-actin was used as a loading control. Each value is the mean ± SD, n = 3. $^{**}P<0.01$ *vs*. the shCtr group.

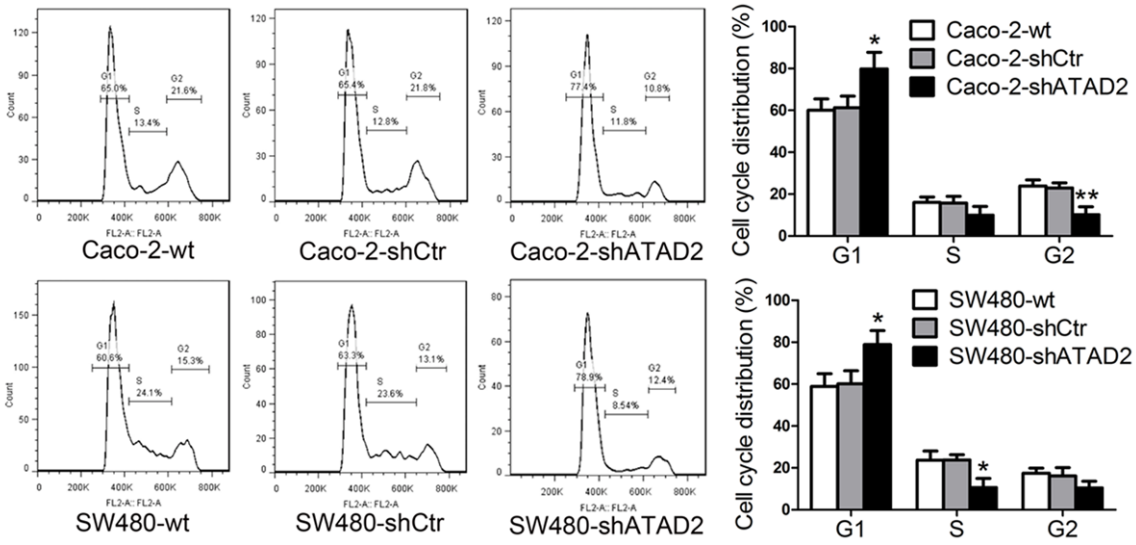

Figure 4. ATAD2 knockdown caused cell cycle arrest at the G1 phase. Caco-2 and SW480 cells transfected with shATAD2 or shCtr plasmid were harvested, stained with PI and analyzed by flow cytometer. Cell cycle distribution was represented using a histogram. Each value is the mean ± SD, n = 3. **P*<0.05 and ***P*<0.01 *vs*. the shCtr group.

ATAD2 knockdown inhibited tumor growth in vivo

To assess the effect of ATAD2 knockdown on tumor growth *in vivo*, SW480 cells transfected with vehicle and shATAD2 plasmid were injected subcutaneously into female nude mice. Tumor sizes were measured every 3 days and tumor tissues were collected on day 28 post-inoculation for further analyses and weighted (**Figure 6A**). Our results demonstrated that tumor volumes in the shCtr group were sharply increased. As expected, tumor volumes (**Figure 6B**) (15 d, *P*<0.05; 18, 21, 24 and 27 d, *P*<0.01) and tumor weights (**Figure 6C**, *P*<0.05) in the shATAD2 group were significantly decreased compared with the shCtr group. In the shATAD2 group, the mRNA levels of ATAD2, PCNA, c-myc and Ki67 in tumor tissues were remarkably downregulated compared with the shCtr group (**Figure 6D**, *P*<0.01). Immunohistochemistry (IHC) further demonstrated the changes of ATAD2 and Ki67 in tumor tissues (**Figure 6E**).

Discussion

Colorectal cancer (CRC) is one of the most malignant cancers in the world [18, 19]. ATAD2 has been reported to be highly expressed in many cancers [20-22]. Previous researches have demonstrated that ATAD2 is associated with the development and progression of malignant cancers [21, 23-26]. However, the biological function of ATAD2 in CRC remains unclear. In our present study, we silenced ATAD2 gene using RNAi technology and firstly evaluated the impact of ATAD2 knockdown on the proliferation of CRC cell lines *in vitro* and *in vivo*.

Proliferation is one of the hallmarks of cancer [27]. Several previous studies have found that ATAD2 participates in many cellular processes, including cell proliferation and migration. Silencing of ATAD2 gene expression in two cervical cancer cell lines HeLa and SiHa using siRNA effectively inhibits their growth and clonogenic potentials [23]. Additionally, ATAD2-RNAi-lentivirus treatment inhibits tumor growth of hepatocellular carcinoma (HCC) *in vivo* in nude mice [10]. In our study, we found that silencing of ATAD2 inhibited the proliferation and colony formation of Caco-2 and SW480 cells and further suppressed tumor growth in BALB/c-nude mice. PCNA is a nuclear protein and is involved in DNA replication. Generally, non-dividing cells express low levels of PCNA, while transforming cells and proliferating cells express high levels of PCNA [28]. Moreover, there is also a correlation between PCNA expression levels and cancer cell proprieties, including malignancy degree and metastasis of tumors. Therefore, it has been commonly used as a marker for tumor growth [29]. c-myc is an oncogene and a member of MYC family [30, 31]. The members of MYC family regulate tumor

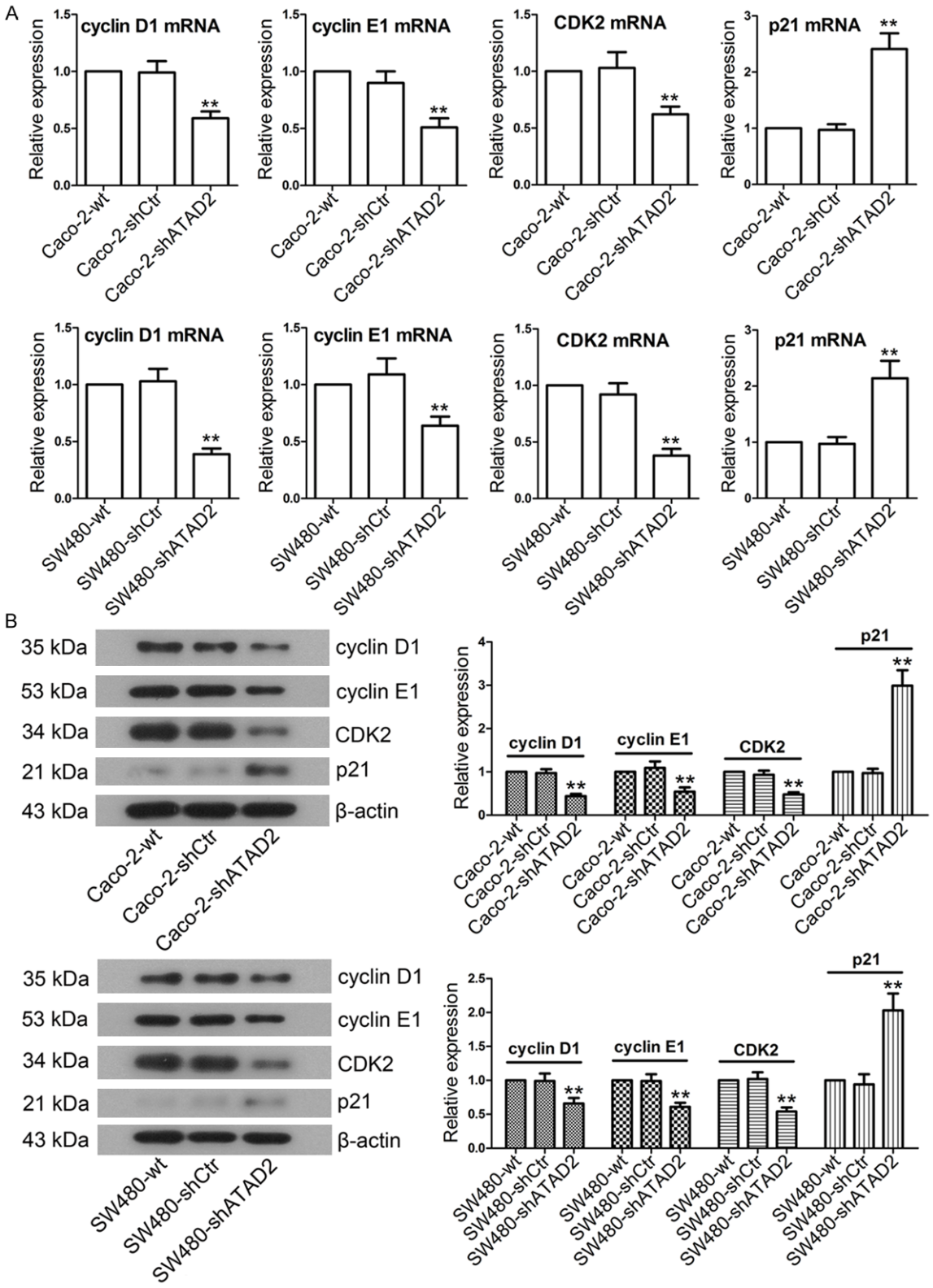

Figure 5. Effect of ATAD2 knockdown on the expression of cell cycle-related genes. A. After shRNA transfection, the mRNA levels of cyclin D1, cyclin E1, CDK2 and p21 were determined by real-time PCR and normalized to β-actin. B. Western blot analysis of cyclin D1, cyclin E1, CDK2 and p21 protein levels in shRNA-transfected Caco-2 and SW480 cells. β-actin was served as an internal control. Each value is the mean ± SD, n = 3. ***P*<0.01 *vs*. the shCtr group.

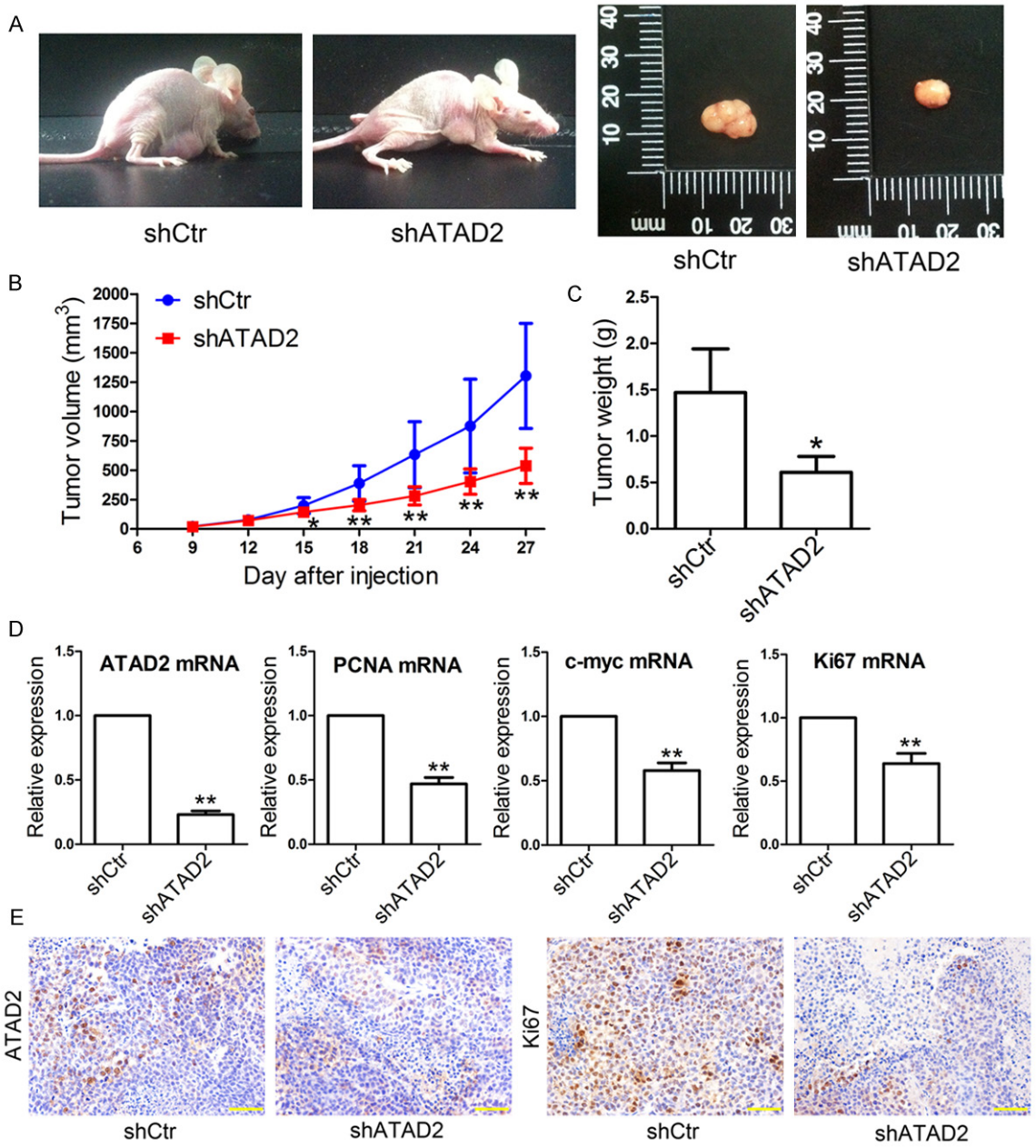

Figure 6. ATAD2 knockdown inhibited tumor growth in BALB/c-nude mice *in vivo* and downregulated the levels of proliferation-related genes in tumor tissues. The 4-6 weeks old female nude mice were subcutaneously injected with 1×10^7 SW480 cells that transfected with shCtr or shATAD2 plasmid. A. Representative images of the mice and tumors. B. Tumor volume was monitored every 3 days using a caliper. C. Twenty-eight days post-inoculation, tumors in mice were excised and then weighted. D. Real-time PCR was performed to detect the mRNA levels of ATAD2, PCNA, c-myc and Ki67. E. ATAD2 and Ki67 protein levels in tumor tissues were measured by IHC. Representative images are shown. Scale bar = 50 μm. Each value is the mean ± SD, n = 3. **P*<0.05 and ***P*<0.01 *vs*. the shCtr group.

cell proliferation and cancer progression in humans [16]. Ki67 antigen is a well-known proliferation marker [32]. It is elevated in multiple cancer cells, including cervical cancer, glioma and breast cancer, reflecting malignant proliferation capability of cancer cells [33]. However, the impact of ATAD2 silencing on the expression of c-myc, PCNA and Ki67 in CRC cells remains unknown. Our current studies showed that knockdown of ATAD2 significantly decreased the expression levels of c-myc, PCNA and Ki67 in cells and tumor tissues. The

results indicate that ATAD2 participate in cell proliferation and tumor growth through regulating the expression of proliferation-related proteins.

Akt is known to be associated with cell proliferation through regulating cell cycle and cell apoptosis [34]. Akt signaling pathway is activated in lung cancer, colon cancer and breast cancer. It has been fully accepted that Akt plays crucial roles in tumor growth and progression [35]. Our study showed that ATAD2 silencing decreased the levels of phosphorylated (p)-Akt in CRC cells, indicating that the inhibition of Akt.

Cell cycle is positively correlated with cyclins and CDKs and negatively correlated with the inhibitors of CDK, such as p21 and p16. Cyclins regulate cell cycle progression through forming complexes with CDKs [36]. p21 can also interact with CDKs and inhibit the activities of CDKs, thereby arresting the cell cycle at G1/S phase or G2/M phase [37]. Both cyclin D1 and c-myc are vital proteins that responsible for the transition of the cell cycle from G1 to S phase [38]. Previous studies have shown that ATAD2 knockdown induces cell cycle arrest of multiple hepatocellular carcinoma (HCC) cell lines *in vitro* [10, 25]. Therefore, we evaluated the effect of ATAD2 silencing on cell cycle progression and the expression levels of cell cycle-related proteins in CRC cell lines. In our study, we found that ATAD2 knockdown induced cell cycle arrest at the G1 phase, greatly downregulated cyclin D1, cyclin E and CDK2 levels, and elevated the expression levels of p21 in both Caco-2 and SW480 cells. The results suggest that ATAD2 inhibit CRC cell proliferation via the induction of cell cycle arrest.

In conclusion, ATAD2 silencing significantly inhibited the proliferation of CRC cells *in vitro*, induced cell cycle arrest and suppressed tumor growth *in vivo*, providing evidences that ATAD2 may serve as an effective therapeutic target for the treatment of CRC.

Disclosure of conflict of interest

None.

Address correspondence to: Dr. Chunyan Zhao, Department of Physiology, College of Basic Medical Sciences, Jilin University, 126 Xinmin Avenue, Changchun 130021, Jilin, China. E-mail: chunyan_zh2012@sina.com; Dr. Lei Wang, Department of Colorectal and Anal Surgery, The First Hospital of Jilin University, 3302 Jilin Road, Changchun 130021, Jilin, China. E-mail: lei_wang2007@yeah.net

References

[1] Ueda K, Hosokawa M and Iwakawa S. Cellular Uptake of Decitabine by Equilibrative Nucleoside Transporters in HCT116 Cells. Biol Pharm Bull 2015; 38: 1113-1119.

[2] Zhao M, Liang F, Zhang B, Yan W and Zhang J. The impact of osteopontin on prognosis and clinicopathology of colorectal cancer patients: a systematic meta-analysis. Sci Rep 2015; 5: 12713.

[3] Yang WJ, Shen XJ, Ma XX, Tan ZG, Song Y, Guo YT and Yuan M. Correlation of human epidermal growth factor receptor protein expression and colorectal cancer. World J Gastroenterol 2015; 21: 8687-8696.

[4] Li J, Liu Y, Wang C, Deng T, Liang H, Wang Y, Huang D, Fan Q, Wang X, Ning T, Liu R, Zhang CY, Zen K, Chen X and Ba Y. Serum miRNA expression profile as a prognostic biomarker of stage II/III colorectal adenocarcinoma. Sci Rep 2015; 5: 12921.

[5] He P, Liang J, Shao T, Guo Y, Hou Y and Li Y. HDAC5 promotes colorectal cancer cell proliferation by up-regulating DLL4 expression. Int J Clin Exp Med 2015; 8: 6510-6516.

[6] Wei ZJ, Tao ML, Zhang W, Han GD, Zhu ZC, Miao ZG, Li JY and Qiao ZB. Up-regulation of microRNA-302a inhibited the proliferation and invasion of colorectal cancer cells by regulation of the MAPK and PI3K/Akt signaling pathways. Int J Clin Exp Pathol 2015; 8: 4481-4491.

[7] Zhang GJ, Li JS, Zhou H, Xiao HX, Li Y and Zhou T. MicroRNA-106b promotes colorectal cancer cell migration and invasion by directly targeting DLC1. J Exp Clin Cancer Res 2015; 34: 73.

[8] Creech GS, Paresi C, Li YM and Danishefsky SJ. Chemical synthesis of the ATAD2 bromodomain. Proc Natl Acad Sci U S A 2014; 111: 2891-2896.

[9] Demont EH, Chung CW, Furze RC, Grandi P, Michon AM, Wellaway C, Barrett N, Bridges AM, Craggs PD, Diallo H, Dixon DP, Douault C, Emmons AJ, Jones EJ, Karamshi BV, Locke K, Mitchell DJ, Mouzon BH, Prinjha RK, Roberts AD, Sheppard RJ, Watson RJ and Bamborough P. Fragment-Based Discovery of Low-Micromolar ATAD2 Bromodomain Inhibitors. J Med Chem 2015; 58: 5649-5673.

[10] Wu G, Lu X, Wang Y, He H, Meng X, Xia S, Zhen K and Liu Y. Epigenetic high regulation of ATAD2 regulates the Hh pathway in human he-

patocellular carcinoma. Int J Oncol 2014; 45: 351-361.
[11] Zou JX, Guo L, Revenko AS, Tepper CG, Gemo AT, Kung HJ and Chen HW. Androgen-induced coactivator ANCCA mediates specific androgen receptor signaling in prostate cancer. Cancer Res 2009; 69: 3339-3346.
[12] Fouret R, Laffaire J, Hofman P, Beau-Faller M, Mazieres J, Validire P, Girard P, Camilleri-Broet S, Vaylet F, Leroy-Ladurie F, Soria JC and Fouret P. A comparative and integrative approach identifies ATPase family, AAA domain containing 2 as a likely driver of cell proliferation in lung adenocarcinoma. Clin Cancer Res 2012; 18: 5606-5616.
[13] Bamborough P, Chung CW, Furze RC, Grandi P, Michon AM, Sheppard RJ, Barnett H, Diallo H, Dixon DP, Douault C, Jones EJ, Karamshi B, Mitchell DJ, Prinjha RK, Rau C, Watson RJ, Werner T and Demont EH. Structure-Based Optimization of Naphthyridones into Potent ATAD2 Bromodomain Inhibitors. J Med Chem 2015; 58: 6151-78.
[14] Chen Y, Gao Q, Huang M, Liu Y, Liu Z, Liu X and Ma Z. Characterization of RNA silencing components in the plant pathogenic fungus Fusarium graminearum. Sci Rep 2015; 5: 12500.
[15] Zou JX, Revenko AS, Li LB, Gemo AT and Chen HW. ANCCA, an estrogen-regulated AAA+ ATPase coactivator for ERalpha, is required for coregulator occupancy and chromatin modification. Proc Natl Acad Sci U S A 2007; 104: 18067-18072.
[16] Ciro M, Prosperini E, Quarto M, Grazini U, Walfridsson J, McBlane F, Nucifero P, Pacchiana G, Capra M, Christensen J and Helin K. ATAD2 is a novel cofactor for MYC, overexpressed and amplified in aggressive tumors. Cancer Res 2009; 69: 8491-8498.
[17] Livak KJ and Schmittgen TD. Analysis of relative gene expression data using real-time quantitative PCR and the 2(-Delta Delta C(T)) Method. Methods 2001; 25: 402-408.
[18] Otero-Estevez O, Chiara LD, Rodriguez-Girondo M, Rodriguez-Berrocal FJ, Cubiella J, Castro I, Hernandez V and Martinez-Zorzano VS. Serum matrix metalloproteinase-9 in colorectal cancer family-risk population screening. Sci Rep 2015; 5: 13030.
[19] Zheng Y, Guo J, Zhou J, Lu J, Chen Q, Zhang C, Qing C, Koeffler HP and Tong Y. FoxM1 transactivates PTTG1 and promotes colorectal cancer cell migration and invasion. BMC Med Genomics 2015; 8: 49.
[20] Hwang HW, Ha SY, Bang H and Park CK. ATAD2 as a Poor Prognostic Marker for Hepatocellular Carcinoma after Curative Resection. Cancer Res Treat 2015; 47: 853-61.
[21] Wan WN, Zhang YX, Wang XM, Liu YJ, Zhang YQ, Que YH and Zhao WJ. ATAD2 is highly expressed in ovarian carcinomas and indicates poor prognosis. Asian Pac J Cancer Prev 2014; 15: 2777-2783.
[22] Zhang Y, Sun Y, Li Y, Fang Z, Wang R, Pan Y, Hu H, Luo X, Ye T, Li H, Wang L, Chen H and Ji H. ANCCA protein expression is a novel independent poor prognostic marker in surgically resected lung adenocarcinoma. Ann Surg Oncol 2013; 20 Suppl 3: S577-582.
[23] Zheng L, Li T, Zhang Y, Guo Y, Yao J, Dou L and Guo K. Oncogene ATAD2 promotes cell proliferation, invasion and migration in cervical cancer. Oncol Rep 2015; 33: 2337-2344.
[24] Shang P, Meng F, Liu Y and Chen X. Overexpression of ANCCA/ATAD2 in endometrial carcinoma and its correlation with tumor progression and poor prognosis. Tumour Biol 2015; 36: 4479-4485.
[25] Wu G, Liu H, He H, Wang Y, Lu X, Yu Y, Xia S, Meng X and Liu Y. miR-372 down-regulates the oncogene ATAD2 to influence hepatocellular carcinoma proliferation and metastasis. BMC Cancer 2014; 14: 107.
[26] Caron C, Lestrat C, Marsal S, Escoffier E, Curtet S, Virolle V, Barbry P, Debernardi A, Brambilla C, Brambilla E, Rousseaux S and Khochbin S. Functional characterization of ATAD2 as a new cancer/testis factor and a predictor of poor prognosis in breast and lung cancers. Oncogene 2010; 29: 5171-5181.
[27] Hanahan D and Weinberg RA. Hallmarks of cancer: the next generation. Cell 2011; 144: 646-674.
[28] Zhang XQ, Huang XF, Mu SJ, An QX, Xia AJ, Chen R and Wu DC. Inhibition of proliferation of prostate cancer cell line, PC-3, in vitro and in vivo using (-)-gossypol. Asian J Androl 2010; 12: 390-399.
[29] Tanaka S, Haruma K, Tatsuta S, Hiraga Y, Teixeira CR, Shimamoto F, Yoshihara M, Sumii K and Kajiyama G. Proliferating cell nuclear antigen expression correlates with the metastatic potential of submucosal invasive colorectal carcinoma. Oncology 1995; 52: 134-139.
[30] Wang AP, Li XH, Yang YM, Li WQ, Zhang W, Hu CP, Zhang Z and Li YJ. A Critical Role of the mTOR/eIF2alpha Pathway in Hypoxia-Induced Pulmonary Hypertension. PLoS One 2015; 10: e0130806.
[31] Vadde R, Radhakrishnan S, Reddivari L and Vanamala JK. Triphala Extract Suppresses Proliferation and Induces Apoptosis in Human Colon Cancer Stem Cells via Suppressing c-Myc/Cyclin D1 and Elevation of Bax/Bcl-2 Ratio. Biomed Res Int 2015; 2015: 649263.
[32] Yuan JP, Wang LW, Qu AP, Chen JM, Xiang QM, Chen C, Sun SR, Pang DW, Liu J and Li Y. Quan-

tum dots-based quantitative and in situ multiple imaging on ki67 and cytokeratin to improve ki67 assessment in breast cancer. PLoS One 2015; 10: e0122734.

[33] Li L, Wang K, Sun X, Sun Y, Zhang G and Shen B. Parameters of dynamic contrast-enhanced MRI as imaging markers for angiogenesis and proliferation in human breast cancer. Med Sci Monit 2015; 21: 376-382.

[34] Yadav V, Varshney P, Sultana S, Yadav J and Saini N. Moxifloxacin and ciprofloxacin induces S-phase arrest and augments apoptotic effects of cisplatin in human pancreatic cancer cells via ERK activation. BMC Cancer 2015; 15: 581.

[35] Attoub S, Arafat K, Kamel Hammadi N, Mester J and Gaben AM. Akt2 knock-down reveals its contribution to human lung cancer cell proliferation, growth, motility, invasion and endothelial cell tube formation. Sci Rep 2015; 5: 12759.

[36] Lv XJ, Zhao LJ, Hao YQ, Su ZZ, Li JY, Du YW and Zhang J. Schisandrin B inhibits the proliferation of human lung adenocarcinoma A549 cells by inducing cycle arrest and apoptosis. Int J Clin Exp Med 2015; 8: 6926-6936.

[37] Abbas T and Dutta A. p21 in cancer: intricate networks and multiple activities. Nat Rev Cancer 2009; 9: 400-414.

[38] Wen HC, Chuu CP, Chen CY, Shiah SG, Kung HJ, King KL, Su LC, Chang SC and Chang CH. Elevation of soluble guanylate cyclase suppresses proliferation and survival of human breast cancer cells. PLoS One 2015; 10: e0125518.